Checkerboard Self-Patterning of an Ionic Liquid Film on Mercury

L. Tamam, B. M. Ocko, H. Reichert, and M. Deutsch

Phys. Rev. Lett. **106**, 197801 — Published 10 May 2011

DOI: 10.1103/PhysRevLett.106.197801

Checkerboard self-patterning of an ionic liquid film on mercury

L. Tamam,[1] B.M. Ocko,[2] H. Reichert,[3] and M. Deutsch[1,*]

[1] *Physics Dept. & Institute of Nanotechnology, Bar-Ilan University, Ramat-Gan 52900, Israel*
[2] *Condensed Matter Physics & Materials Sciences Dept., Brookhaven National Lab, Upton NY 11973*
[3] *European Synchrotron Radiation Facility, P.O. Box 220, 38043 Grenoble, France*

Å-resolution studies of room temperature ionic liquid (RTIL) interfaces are scarce, in spite of their long-recognized importance for the science and many applications of RTILs. We present an Å-resolution x-ray study of a Langmuir film of an RTIL on mercury. At low (high) coverage [90 (50) Å^2/molecule] a mono-(bi-)layer of surface-parallel molecules are found. The molecules self-assemble in a lateral ionic checkerboard pattern, unlike the uniform-charge, alternate-ion layers of this RTIL at its bulk/solid interface. A 2D-smectic order is found, with molecules packed in parallel stripes, forming long-range order normal to, but none along, the stripes.

RTILs are a novel class of liquids, consisting solely of ions without a solvent. The bulky and irregular shape of the ions, often comprising hydro- and fluoro-carbon chains and rings, inhibits solidification even at room temperature in spite of the strong Coulomb interaction [1]. Their favourable chemical properties, such as [1, 2] non-volatility, wide electrochemical window, high ion mobility, etc. renders them outstanding "green" replacements for volatile, corrosive and polluting solvents, reaction media, and working fluids in the chemical industries [1], and in energy- and electronics-related applications in batteries, solar and fuel cells [3], and MEMSs [4].

The intense scientific interest in RTILs stems from their complex combination of interactions, van der Waals, Coulomb, dipole, and hydrogen bonding, rarely occurring simultaneously in other materials [5, 6]. Being infinite-concentration ionic "solutions", RTILs are strongly correlated systems, going beyond the validity regime of the Poisson-Boltzman equation, and the Gouy-Chapman and Stern models of the electric double layer [7], and thus allowing insight into this scarcely studied regime. Theoretical progress in understanding the interplay of interactions in, and of the strong-correlation aspects of, RTILs is hampered by the scarcity of molecular-resolution structural data, particularly at interfaces, where such measurements are highly challenging. While a few such studies of liquid/vapour (*l/v*) RTIL interfaces are available [8, 9], only two address liquid/solid (*l/s*) interfaces [10, 11]. No bulk liquid/liquid (*l/l*) interface studies were published. Even these handful of studies address only interfaces between bulk phases. No Å-resolution structure of 2D Langmuir films (LFs) have been published to date for any RTIL, even though numerous studies of LFs on water- [12–14] and mercury [15–17] of non-RTIL compounds demonstrate the deep insights obtainable from such measurements. In particular, LF x-ray measurements can determine the surface-parallel structure and its coverage dependence. These are masked in *l/s* and *l/l* interface studies by the strong bulk scattering.

We present here an Å-resolution x-ray study of the structure of a liquid-mercury supported RTIL LF, 1-butyl- 1-methylpyrrolidinium tris(pentafluoroethyl) tri-

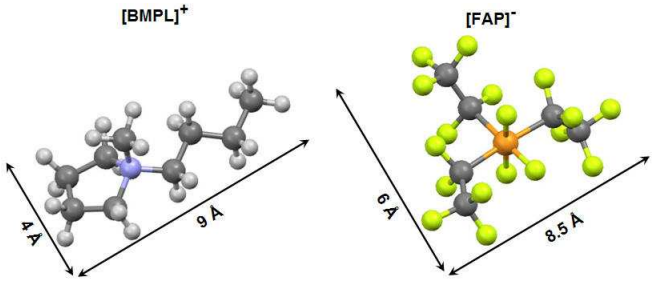

FIG. 1. Configurations and dimensions of the ions.

fluorophosphate ($[BMPL]^+[FAP]^-$). The surface-parallel molecules self-organize into stripes, which exhibit one-dimensional, smectic-like order, implying a checkerboard-like ionic surface tiling. This is consistent with the expected domination of the lateral order by the strong ionic Coulomb interaction, but differs from the ordering found for the bulk of the same RTIL at a charged solid interface, where alternately-charged ion layering was observed [10].

The energy-optimized calculated $[BMPL]^+$ and $[FAP]^-$ ion configurations (Fig. 1) yield areas of 36 and 51 Å^2 [18]. The measured surface pressure(π)/molecular area(A) isotherm [15, 16] (for method see [19]) is shown in Fig. 2. The steep rise at ∼90 Å^2/molecule marks the point where the molecules of the $A \gg 90$ Å^2/molecule 2D gas start touching, forming a densely packed monolayer [13, 15]. Fits (dashed lines) by the Volmer [20] and van der Waals [21] state equations of an ideal 2D gas of finite-area (A_0) molecules yield exclusion areas $A_0^V = 93$ Å^2/molecule and $A_0^{vdW} = 88$ Å^2/molecule, respectively. The close coincide of the measured A_0 with the sum of areas of the two ions, 87 Å^2/molecule, suggests that the ions comprising the molecule lie flat, side by side, on the mercury surface (Fig. 2, inset), not on top of each other, thus maximizing the vdW contacts of the molecule with the surface. Surface-parallel ion orientations are also found in simulations of similar RTILs, albeit on graphite [22]. This ionic arrangement has a zero net local and global charge, and a lower free energy than that of the alternating uniformly charged

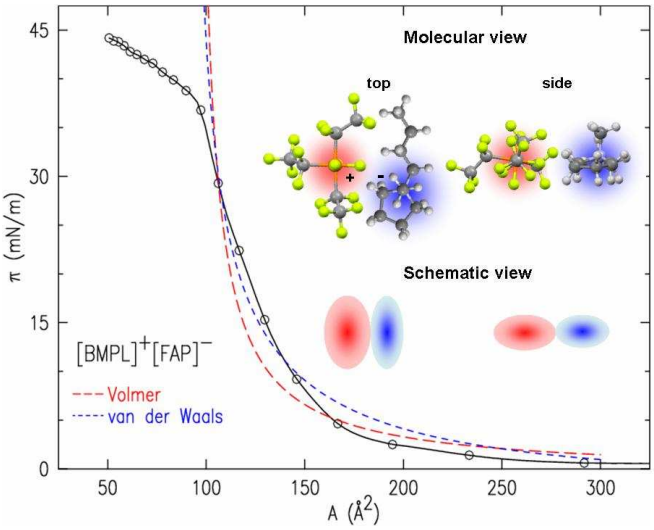

FIG. 2. Measured (symbols and eye-guiding solid line) and fitted(dashed lines) $\pi - A$ isotherm of the mercury-supported RTIL LF, spread from an acetonitrile solution. Inset: schematic of the ions' arrangement on the surface.

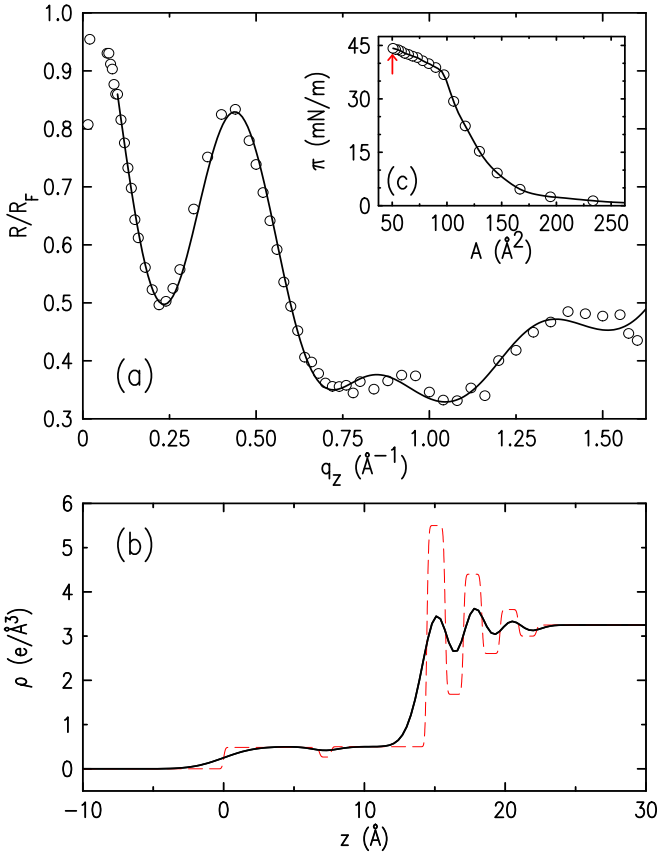

FIG. 3. (a) Fresnel-normalized measured (symbols) and model fitted (line) XR curve. (b) Fit-derived surface normal electron density profile, $\rho(z)$, with (solid line) and without (dashed line) CW roughness smearing. (c) $\pi - A$ isotherm. The arrow marks the measurements' $A = 50$ Å^2/molecule.

layers found at the same RTIL's bulk interface with a charged sapphire substrate [10]. The average of the fitted exclusion areas, $\overline{A}_0 = 90.5$ Å^2/molecule, and the molar volume, 0.370 l/mol, yield a monolayer thickness $\overline{d}_0 = 6.8$ Å, supported by the x-ray results below.

Two additional isotherm features should be noted. First, the linear sloping plateau at $A < A_0$ resembles that observed at the same A-range for a mercury-supported stearic acid LF [15], which was shown to correspond to a continuous conversion with decreasing A of a monolayer to a bilayer of surface-parallel molecules. Second, no sharp rise, the sign of a transition from lying-down to standing-up molecules, is observed near film collapse at $A \leq 50$ Å^2/molecule, in contrast with mercury-supported LFs of fatty acids, thiols, and alcohols [15, 16], which show such transitions. These isotherm-derived inferences are confirmed by our x-ray measurements, discussed next.

Since RTILs resist ordering, as their low melting temperatures demonstrate, our x-ray measurements (for methods see [19]) were done at the highest π below film collapse, at $A \approx \overline{A}_0/2 = 50$ Å^2/molecule, where order is most likely to emerge. The x-ray reflectivity (XR), $R(q_z)$, was measured at beamline X22B, NSLS, Brookhaven National Laboratory, USA, as a function of the incoming beam's grazing angle of incidence onto the surface, α, where $q_z = (4\pi/\lambda)\sin\alpha$, and $\lambda = 1.5127$ Å is the x-rays' wavelength [23, 24]. The interface's structural information resides in the deviations of $R(q_z)$ from $R_F(q_z)$, the theoretical Fresnel XR of an ideally smooth and abrupt interface. Fig. 3(a) shows the measured (symbols) and box model fitted (line) $R(q_z)/R_F(q_z)$. The model, successfully used for numerous LFs of organic molecules on mercury [15, 16, 25], uses 6 slabs to mimic the decaying layering of mercury at the interface [26–28]. As the measurements were done at 50 Å^2/molecule, half the area of a flat-lying molecule, a bilayer was expected, as discussed above. To reproduce well (Fig. 3(a), line) the complex $R(q_z)/R_F(q_z)$ measured (Fig. 3(a), symbols) three slabs were necessary to describe the RTIL layer covering the mercury surface: two identical slabs of fixed nominal density $\rho = 0.485$ e/Å^3 (calculated from the molecular volume and number of electrons) and thickness, 6.8 Å, separated by a low-density layer (LDL) ~ 1 Å thick and $\rho = 0.27$ e/Å^3 dense. The best-fit surface-normal electron density profile, $\rho(z)$, is shown in Fig. 3(b) with (solid line) and without (dashed line) the smearing by roughness due to the thermally-excited capillary waves (CW), decorating all liquid interfaces [29, 30]. The good fit in Fig. 3(a) supports, therefore, the two-layer structure of flat-lying molecules inferred above from the isotherm.

To elucidate the surface parallel order within the layer, grazing incidence diffraction (GID) measurements [23, 24] were done at 50 Å^2/molecule. Here a small incidence angle α is used and the detector is scanned out of the reflection plane by an angle 2θ, to yield a finite surface-

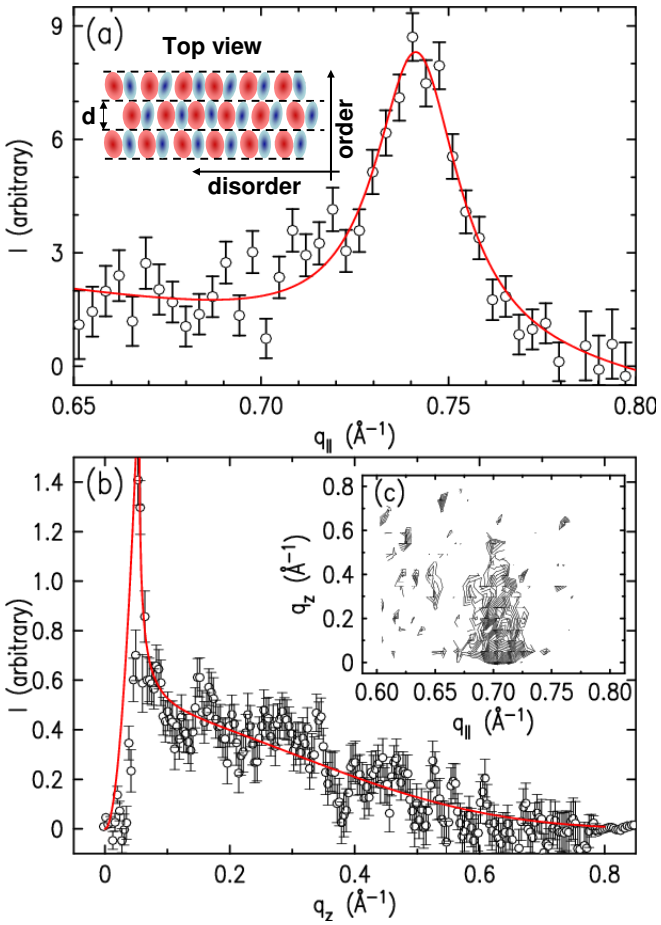

FIG. 4. (a) Measured (symbols) and Lorentzian-plus-linear background fitted (line) GID peak at $A = 50$ Å^2/molecule. Inset: Schematic top view of the ionic order, discussed in the text. (b) Measured BR (symbols) and theoretical fit (line) at the GID peak. (c) Contour plot of the measured BR.

parallel diffraction vector $q_\parallel \approx (4\pi/\lambda)\sin\theta$. An extensive search revealed only a single GID peak (Fig. 4(a)) at $q_\parallel^0 = 0.742$ Å^{-1}, which corresponds to a repeat distance of $d = 2\pi/q_\parallel^0 = 8.47$ Å, suggestively close to the 8.5-9 Å lengths of both $[\mathrm{BMPL}]^+$ and $[\mathrm{FAP}]^-$ (Fig. 1). A single GID peak implies either an hexagonal [13, 24, 31] or a one-dimensional [15] lateral order. The former occurs only rarely in 2D packing of molecules of non-circular surface-parallel cross-sections, such as our RTIL. Moreover, an hexagonal packing with our $q_\parallel^0$ implies an area of $4\sqrt{3}\pi^2/(q_\parallel^0)^2 = 124$ Å^2/molecule, 40% larger than the $A_0 \approx 90$ Å^2/molecule observed in the isotherm, a value supported strongly also by the density needed to fit the measured $R(q_z)/R_F(q_z)$. Thus, a lateral hexagonal order is highly unlikely in our LF.

The second possibility, a one-dimensional order, is consistent with a the molecular area of ~ 90 Å^2/molecule inferred from the isotherm and the XR results. This packing motif is shown schematically in the inset of Fig. 4(a): alternately-charged ions assemble (without positional order) into long stripes. The extended stripes (longitudinally shifted relative to each other, see below) lie side by side, forming long-range order in the stripe-normal direction. $q_\parallel^0$ corresponds to the positional order of the stripes, with a repeat distance equal to the stripe's width, ~ 8.5 Å, close to the ions' length. The absence of long-range positional order *along* the strip, is explainable by small random variations in the azimuthal molecular orientations along the stripe, due to the irregular molecular shape. A very similar ordering was found for LFs of intermediate-length (∼18 carbons) fatty acid molecules on mercury, in their lying-down phase [15]. There, linear carboxyl-bound dimers aggregate to form stripes, with dimers lying stripe-normal at random positions along the stripe. The parallel-lying stripes exhibit stripe-normal positional order with a repeat distance equal to the dimers' length, 52.3 Å for octadecanoic acid [15]. Note however that for fatty acids the structure-dominating inter-dimer interaction is purely dispersive, unlike here, where the interionic Coulomb interaction dominates the structure. Also, the requirement of minimizing the overall Coulomb energy induces a roughly half-molecule longitudinal shift between adjacent stripes to create the lowest-Coulomb-energy checkerboard-like motif, albeit with long-range order in one direction only. A recent study of another RTIL, $[\mathrm{TOMA}]^+[\mathrm{C_4C_4N}]^-$, reports also a checkerboard-like ion arrangement at the bulk *l/v* interface, without, however, any indication for a lateral long-range order in any direction [9].

The crystalline coherence length, ξ, is obtained from the Debye-Scherrer formula, $\xi = 0.9 \times 2\pi/(\Delta^2 q_\parallel - \Delta_{res}^2)^{1/2}$, where $\Delta q_\parallel = 0.0274$ Å^{-1} is the GID peak's full width at half maximum, and $\Delta_{res} = 0.008$ Å^{-1} is the diffractometer's resolution. The poor crystallinity obtained, $\xi \approx 200$ Å only, is in line with the RTILs dominant property of resisting crystallization. The poor crystallinity is also reflected in the low intensity of the GID peak and of the Bragg rod (BR), discussed next.

The BR [24], the surface-normal q_z-distribution of the diffracted intensity at $q_\parallel^0$, provides further information on the ordered molecules. It is shown in Fig. 4(b,c). The intensity contour plot in Fig. 4(c) is typical of a surface layer comprising laterally ordered untilted molecules. The measured BR (Fig. 4(b), symbols) exhibits a surface enhancement peak at 0.055 Å^{-1}, indicating that the GID peak originates in a surface, rather than a bulk, structure. A model (solid line) assuming a *mono*layer of 6.8 Å high molecules untilted from the surface normal is consistent with the measured curve. As both XR and isotherm show the layer at this coverage to be a *bi*layer, the BR result indicates either that while both layers of the film are ordered, the crystallites in one monolayer are out of registration with those of the other, or that one of the monolayers is disordered and the GID peak origi-

nates in a single monolayer only. The present data does not allow distinguishing between these two possibilities. We note however, that simulations, albeit for a different RTIL ($[BMIM]^+[PF_6]^-$) and a different substrate (ordered solid graphite) [22, 32] indicate that for an RTIL multilayer on graphite the interface-adjacent RTIL layer is laterally more ordered than (the two) subsequent ones observed, which somewhat supports the first possibility. On the other hand, the Coulomb repulsion between like charges places a high energetic penalty on the registration of crystallites in the upper and lower layer. The full elimination of this penalty is achievable by a lateral shift of the upper and lower layers to yield a perfect oppositely-charged vertical ion registration. This, however, is achievable only with fully-ordered layers, rather than the 1D order found here. Thus, in our case, the frustration due to the interlayer Coulomb interaction would destroy the (shifted) registration and the BR would reflect a single-layer order only, even when both layers are ordered. This frustration may also account, at least partially, for the small ξ and low intensity of the GID peak and BR. In the corresponding bilayer phase of medium-length fatty acids, discussed above, where the strong Coulomb interaction is absent, a registration of the layers does occur, and is reflected in a twice shorter BR [15].

In conclusion, we have demonstrated here that x-rays can resolve the Å-scale structure of an RTIL LF in both the lateral and longitudinal directions. The structure found here, a checkerboard pattern ordered in one direction only, has similarities with, but also differences from, previously studied structures of mercury-supported fatty acid LFs. In those LFs full 2D lateral order eventually emerges upon increasing the length of the alkyl moiety. Whether a similar order emerges in our RTIL upon increasing its alkyl tail length, in spite of the irregular ionic shapes and the strong Coulomb interaction, remains to be investigated. The dichotomy between the electrically neutral mono- and bi-layers observed here and the alternating, uniformly charged, (multi)layers formed at the charged sapphire interface in contact with a bulk of the *same* RTIL [10] also deserves further investigation, to elucidate the role of the overlying RTIL bulk and the level of substrate charging in the structure formation and characteristics. Above all, a greater body of experiments on LFS of other RTILs, over a broad size and molecular architecture range, is required to broaden and deepen the insights, gleaned from this first study, on the interactions dominating the structure of RTILs at interfaces.

We thank the US-Israel Binational Science Foundation, Jerusalem, for support, and NSLS, Brookhaven National Laboratory (supported by DOE contract DE-AC02-76CH0016) for beamtime.

* E-mail: moshe.deautsch@biu.ac.il

[1] H. Wasserscheid and T. Welton, eds., *Ionic Liquids in Synthesis*, 2nd ed. (Wiley-VCH, 2007).
[2] R. D. Rogers and K. R. Seddon, Science, **302**, 792 (2003).
[3] S.Y. Lee et al., J. Am. Chem. Soc., **132**, 9764 (2010).
[4] I.B. Malham et al, Soft Matt. **6**, 4062 (2010).
[5] L. Crowhurst et al, J. Am. Chem. Soc. **126**, 11549 (2004).
[6] H. Weingärtner, Angew. Chem. Int. Ed., **47**, 654 (2008).
[7] M.Z. bazant et al, Phys. Rev. Lett., **106**, 046102 (2011).
[8] E. Sloutskin et al., J. Am. Chem. Soc., **127**, 7796 (2005).
[9] N. Nishi et al., J. Chem. Phys., **132**, 164705 (2010).
[10] M. Mezger et al., Science, **322**, 424 (2008).
[11] M. Mezger et al., J. Chem. Phys., **131**, 094701 (2009).
[12] S.G. Wolf et al., Nature, **328**, 63 (1987).
[13] V.M. Kaganer et al, Rev. Mod. Phys., **71**, 779 (1999).
[14] E. Sloutskin et al., Phys. Rev. Lett., **99**, 136102 (2007).
[15] H. Kraack et al., Science, **298**, 1404 (2002).
[16] B.M. Ocko et al., Phys. Rev. Lett., **94**, 017802 (2005).
[17] L. Tamam et al., Langmuir, **25**, 5111 (2009).
[18] Files Pyr14.pdb & (C2F5)3PF3.pdb, www.il-eco.uft.uni-bremen.de.
[19] See EPAPS Doc. XXX for the supplemental material.
[20] M. Volmer, Z. Phys. Chem. (Leipzig), **115**, 253 (1925).
[21] J. Israelachvili, *Intermolecular and surface forces*, 2nd ed. (Academic Press, London, UK, 1992).
[22] S.A. Kislenko et al, Phys. Chem. Chem. Phys. **11**, 5584 (2009).
[23] J. Als-Nielsen and D. McMorrow, *Elements of Modern X-ray Physics* (Wiely, New York, USA, 2001).
[24] B.M. Ocko et al., Phys. Rev. E, **55**, 3164 (1997).
[25] L. Tamam et al., Soft Matt., **6**, 526 (2010).
[26] O.M. Magnussen st al., Phys. Rev. Lett., **74**, 4444 (1995).
[27] A. Elsen et al., Phys. Rev. Lett., **104**, 105501 (2010).
[28] L. Tamam et al., J. Phys. Chem. Lett., **1**, 1041 (2010).
[29] B.M. Ocko et al., Phys. Rev. Lett., **72**, 242 (1994).
[30] P. S. Pershan, J. Phys. Chem. B, **113**, 3639 (2009).
[31] X.Z. Wu et al., Phys. Rev. Lett., **70**, 958 (1993).
[32] M. Sha et al., J. Chem. Phys., **128**, 134504 (2008).